Application of Emission Source Microscopy Technique to EMI Source Localization above 5 GHz

Pratik Maheshwari, Victor Khilkevich, David Pommerenke
Missouri University of Science and Technology
Rolla, USA
prm8c7, khikevichv, davidjp@mst.edu

Hamed Kajbaf, Jin Min
Amber Precision Instruments
Sunnyvale, California
hamed, jinmin@amberpi.com

***Abstract* - This paper presents the utilization of the emission source microscopy (ESM) technique to localize active sources of radiation on a PCB. For complex and large systems with multiple sources, localizing the sources of radiation often proves difficult. Near-field scanning provides limited information about the components contributing to far-field radiation. Two-dimensional synthetic aperture radar, a well-known technique used to diagnose and align phase array antennas, is adapted as emission source microscopy and utilized here for this alternative application. This paper presents the source localization methodology, along with simulation and measurement results. The results show that the proposed method can detect multiple active sources on a complex PCB.**

Keywords — source localization; EMI; emission source microscopy; SAR; near-field scanning.

I. INTRODUCTION

Near-field electromagnetic scanning often is used for root cause diagnosis by determining near-field radiation patterns and coupling mechanisms. Near-field scanning may provide information about the surface current, tangential fields and the reactive near-field distribution on the device under test (DUT). The near-field contains both evanescent and propagating fields. The evanescent waves are dominant, which may lead to the misinterpretation of the dominant sources contributing to the far-field. In practice, however, engineers mainly are concerned about only the sources of electromagnetic interference (EMI) contributing to far-field radiation. To identify these sources, engineers must depend upon their experience or trial and error. Another limitation of near-field scanning is that the probe may not be able to access all locations near the PCB due to the complex geometry and high component density. This leads to the incorrect measurement of fields at different vertical distances from the PCB. One advantage of near-field scanning is that it can achieve better resolution depending upon the scanning step and the probe size.

To overcome the limitations of near-field scanning in locating EMI radiation sources, the emission source microscopy presented in this paper can be used to determine the sources of far-field radiation. In the literature, the investigators in [1] discussed a similar idea for detecting faulty antennas in antenna arrays. They performed two phase-synchronized near-field measurements before applying the synthetic aperture radar (SAR) algorithm to detect faulty antennas. SAR techniques are used mainly for antenna diagnostics and antenna pattern measurements [2]. Such techniques also have been used for microwave imaging to detect concealed objects and structural defects [3]-[5]. Standard SAR methods use signals reflected from a target and received by a scanning antenna to reconstruct the target's image. The method proposed in this paper uses a 2D ESM algorithm based on the SAR technique to detect active sources of radiation on a complex PCB. The fields from the active radiation sources, along with the amplitude and phase, are measured on a planar surface away from the DUT. The ESM algorithm is applied to propagate the fields back to the source plane and to localize the source of radiation. The method is presented using an analytical formulation and validated using both full-wave simulations and measurements.

II. EMISSION SOURCE MICROSCOPY ALGORITHM

A. Analytical formulation of 2D ESM algorithm

To apply the ESM algorithm, the fields from the sources are measured on a planar surface approximately two to three wavelengths from the DUT in order to be outside the DUT's reactive near-field and to achieve the minimal effect of the probe on the DUT's fields. Observing the field pattern on the planar scanning field yields very limited information about the location and number of radiation sources.

The measured fields on the observation plane can be expanded using plane wave spectrum theory, which states that any monochromatic but otherwise arbitrary wave can be represented as a superposition of plane waves travelling in different directions with different amplitudes but the same frequency. According to [6], the electric field intensity in a charge-free region on a plane $(x, y, 0)$ can be represented as a superposition of plane waves in the form of Fourier transform,

$$E(x,y,0) = \frac{1}{4\pi^2}\int_{-\infty}^{\infty}\int_{-\infty}^{\infty} f(k_x,k_y,0)e^{-j(k_x x+k_y y)}dk_x dk_y \quad (1)$$

$$E(x,y,0) = F^{-1}(f(k_x,k_y,0))$$

where $f(k_x,k_y,0)$ is the 2-dimensional Fourier transform of $E(x,y,z)$, as given by,

$$f(k_x,k_y,0) = \int_{-\infty}^{\infty}\int_{-\infty}^{\infty} E(x,y,0)\, e^{j(k_x x+k_y y)}dxdy \quad (2)$$

$$f(k_x, k_y, 0) = F(E(x, y, 0))$$

Here, k_x and k_y are the spectrum wavenumbers in the x and y directions, respectively, and F and F^{-1} are the forward and reverse Fourier transform operators, respectively. It has been shown [7] that the spectrum of the field on any plane parallel to $(x, y, 0)$ can be found using,

$$f(k_x, k_y, z) = f(k_x, k_y, 0) * e^{-jk_z z} \quad (3)$$

where $k_z = \sqrt{{k_0}^2 - {k_x}^2 - {k_y}^2}$ is the planar wave dispersion relation, $k_0 = 2\pi/\lambda$ is the free-space wavenumber, and λ is the wavelength of the active source of radiation.

Therefore, if the field on the plane (x, y, z) is known, the field on the plane $(x, y, 0)$ can be found using,

$$E(x, y, 0) = F^{-1}[F(x, y, z) * e^{-jk_z z}] \quad (4)$$

where 'z' is the vertical distance of the scanning plane from the source plane.

Equation 4 allows back-propagation of the field on one plane to another. If the fields are measured on the plane parallel to the antenna aperture or any other planar source, (4) then the fields on the source plane can be reconstructed. In reality, the fields are not available in the form of continuous functions, as in (1) and (2), but instead are sampled at discrete locations. In the case of uniform sampling, (4) would result in discrete rather than continuous Fourier transforms. Equation (4) serves as the basis of the 2-D ESM algorithm.

In principle, the fields $E(x, y, z)$ can be obtained simultaneously using antennas or probe arrays [8]; however, this is difficult to achieve. A more practical approach is to use a moving probe or antenna and sample the field sequentially from point to point. In this case, the scanning plane can be thought of as a synthetic aperture of a big antenna, or radar. This will, however, limit the method to identifying time-harmonic sources. The rectangular scanning plane is divided into a grid of N x M points. The sampling points on the scanning grid are chosen to be less than $\lambda/2$ in order to satisfy the Nyquist spatial sampling criterion [9]. Although the Nyquist rate is not required for reconstruction, uniformly sampling data at the Nyquist rate reduces the overall complexity of the reconstruction algorithm [10]. At grid sample points, the tangential electric field components E_x and E_y are measured.

The resolution of scanning, height of the scanning plane, and frequency of operation affects the final resolution of the reconstructed image. From optics [11], the numerical aperture of the lens is given as,

$$N.A. = n * \sin\theta \quad (5)$$

where 'n' is the refractive index of the medium, and θ is one-half of the aperture angle in radians, as shown in Fig. 1. Here, 'd' represents the length of the smallest side in meters, and 'h' is the height of the scanning plane above the DUT in meters. Based on the numerical aperture in (5), the resolution of the reconstructed image can be given as,

$$R = \lambda/(2 * N.A.) \quad (6)$$

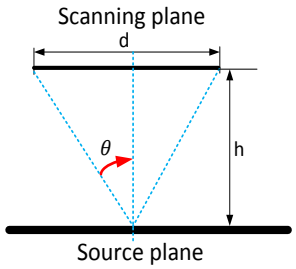

Fig. 1. Aperture angle given by the span of the scan plane

This limits the resolution that can be achieved in the reconstructed image. For an infinitely wide scanning plane, the aperture angle would be 90 degrees, and with air as the medium, the maximum N.A. would be 1. This limits the maximum resolution to $\lambda/2$.

B. Method validation on a PCB

In order to assess the usefulness of the ESM method for EMC applications, a custom PCB with several patch antennas and transmission lines was built. Fig. 2 shows the full-wave model of the PCB built in the CST microwave studio full-wave simulator [12]. The model was built so that the experimental and simulation results could be compared. The patches and traces on the PCB could be excited and terminated individually or simultaneously using a resistive splitter. The PCB was 254 mm x 152 mm, with bigger patches of 20 mm on each side. The ground plane was set as perfect electric conductor (PEC) in the simulation, and the dielectric material between the trace and the ground plane was FR-4 with ε_r 4.3. The simulation was performed at 8.2 GHz.

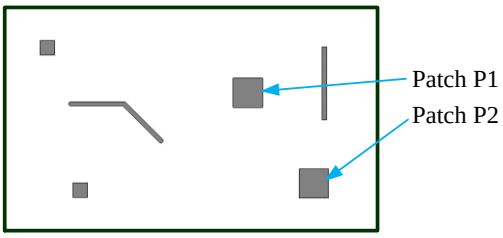

Fig. 2. Model of the custom PCB

The planar field amplitude and phase data were recorded on a rectangular plane above the PCB. The scanning resolution of the rectangular plane was 5 mm, which satisfies the Nyquist spatial sampling criteria. To validate the method, patches P1 and P2 were excited simultaneously. Using the time-domain solver in CST, the tangential electric fields E_x and E_y were sampled at a height of 5 cm above the DUT, as shown in Figs. 3 and 4.

The image of the PCB was overlapped and aligned with the image of the scanned fields to allow an observation of the underlying physical sources of radiation. As Figs. 3 and 4

indicate, no particularly useful information about the source of radiation was obtained by observing the scanned fields. However, when the ESM algorithm given in (4) was applied to the scanned fields, and the reconstructed field on the PCB plane was obtained, the sources were localized easily. The reconstructed fields on the source plane for both orientations appear in Figs. 5 and 6.

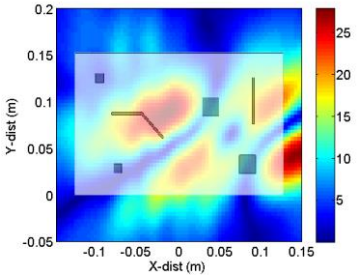

Fig. 3. Scanned E_x magnitude (V/m) field on a rectangular plane at 5 cm above DUT using full-wave simulation

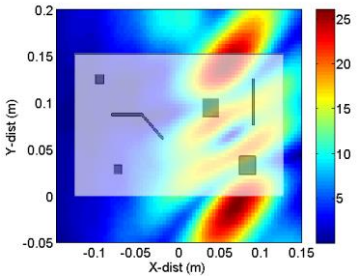

Fig. 4. Scanned E_y magnitude (V/m) field on a rectangular plane at 5 cm above DUT using full-wave simulation

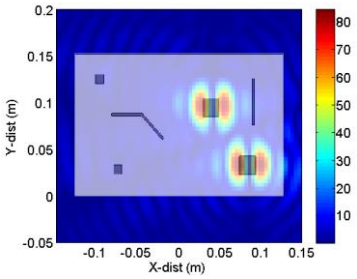

Fig. 5. Reconstructed E_x field magnitude (V/m) on the source plane

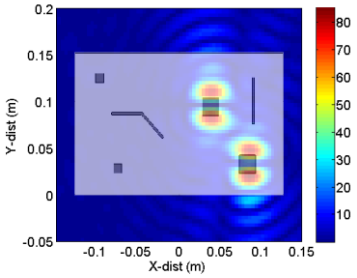

Fig. 6. Reconstructed E_y field magnitude (V/m) on the source plane

The resolution of the reconstructed image, as calculated using (6), was 1.9 cm. The ripples in the reconstructed images around the sources were caused by the truncation of the fields in the spatial domain during the measurement and are actually diffraction rings, which are common in optical microscopy.

For measurement, an open-ended waveguide with a working range of 8.2-12.4 GHz was used as a scanning antenna. It was held and moved in a uniform rectangular grid over the custom PCB using an API 3-axis EMI scanning system [13]. The patches were excited at 8.2 GHz. A vector network analyzer (VNA) was used to measure the amplitude and phase of the scanned fields. Port 1 of the VNA fed a resistive splitter to excite patches P1 and P2, while Port 2 of the VNA was connected to the scanning antenna to receive the signal. The S21 measurement of the VNA provided the amplitude and phase of the fields over the scanning plane. The scanning area was much smaller than in the simulation due to the limited range of the scanning system. The scanned fields from the measurement over the PCB for both orientations appear in Figs. 7 and 8.

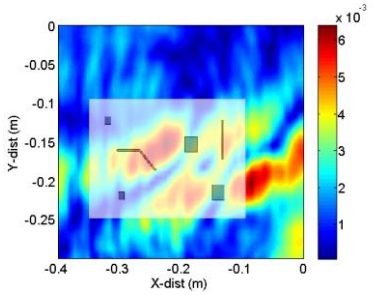

Fig. 7. Measured E_x field magnitude |S21 | on a rectangular plane at 5 cm above the DUT

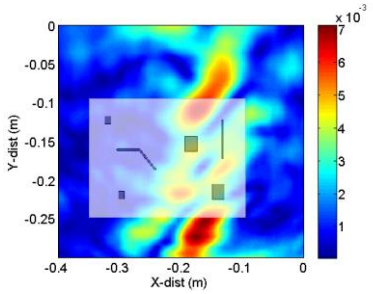

Fig. 8. Measured E_y field magnitude |S21 | on a rectangular plane at 5 cm above the DUT

After applying the ESM algorithm on the measured data and reconstructing the image from the source plane, the sources were identified in both orientations, as in the simulation, as shown in Figs. 9 and 10.

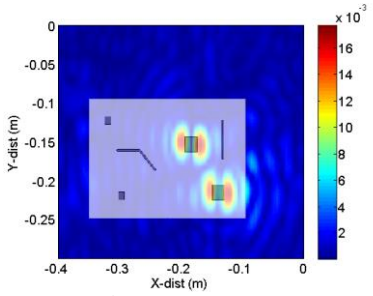

Fig. 9. Reconstructed $\boldsymbol{E_x}$ field magnitude on the source plane

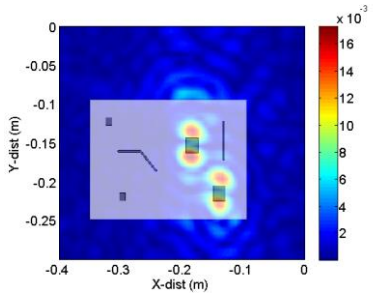

Fig. 10. Reconstructed $\boldsymbol{E_y}$ field magnitude on the source plane

C. *Source localization on an FPGA SI trans-receiver board*

For real DUT, such as FPGA boards, routers, etc., both the scanned amplitude and the phase must be measured. A VNA can be operated in the tuned receiver mode with the internal RF source turned off. In this mode, the VNA can measure the individual amplitudes and phase difference between the inputs. For a real hardware board, such as an FPGA board, a reference signal to one port of the VNA can be obtained either by tapping the signal from the board or using a stationary reference antenna. The other port of the VNA can be used as an input from the scanning antenna. For the FPGA board, the differential clock signal was output on two SMA connectors as shown in Fig. 11. The reference was obtained by tapping the signal from one of the lines of the FPGA clock's differential pair while keeping the other signal line open. The diagram of the phase-resolved measurement setup appears in Fig. 12.

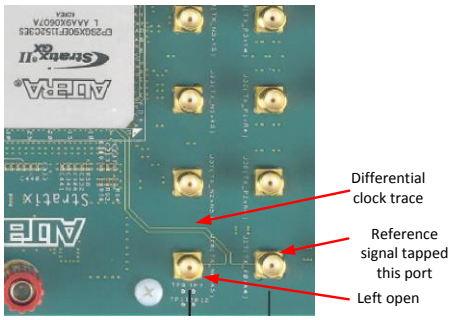

Fig. 11. Actual FPGA board structure

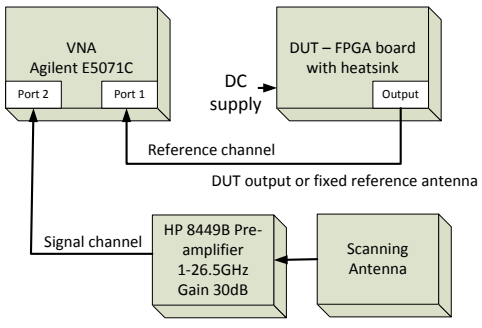

Fig. 12. Phase measurement methodology

The FPGA was programmed to output a pseudorandom bit sequence at one of the differential channels. The clock frequency for the FPGA was 3.125 GHz. The spatial resolution at the clock frequency calculated using (6) was 5 cm, which might be not enough to determine the location of the source on the FPGA board; therefore, the third harmonic, 9.375 GHz, which gave the maximum resolution of 1.56 cm, was used to conduct the experiment. The scanning antenna employed was the open-ended waveguide with a working range of 8.2-12.4 GHz connected on the moving arm of the API 3-axis EMI scanning system [12]. The scanning step was kept at 7 mm in both the x and y directions. The measured field magnitude for Ex component at a height of 5 cm above the FPGA board appear in Fig. 13. As observed, no useful information about the sources of radiation could be obtained from the scanned fields.

Also near-field scan with a scanning step of 3 mm was performed using a near-field magnetic loop probe at 0.5 mm above the PCB surface. Here as compared to the ESM measurement only the magnitude needs to be measured. The result of near-field scanning is shown in Fig. 14. As observed in the near-field scan the active differential trace is observed. Here the fields include both the evanescent wave components and the radiating components and detection of the radiation source is problematic. Next using the fields measured at 5 cm away from the DUT, ESM technique is applied and fields are back-propagated to the PCB plane. The total reconstructed fields on the PCB plane appear in Fig. 15.

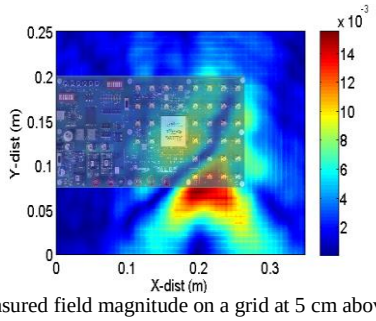

Fig. 13. Measured field magnitude on a grid at 5 cm above the DUT

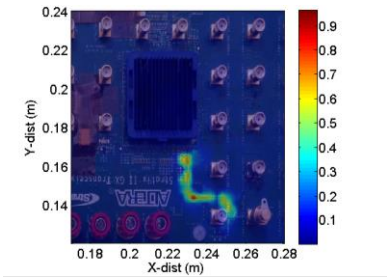

Fig. 14. Measured tangential fields (magnitude) for the FPGA board using near-field scanning

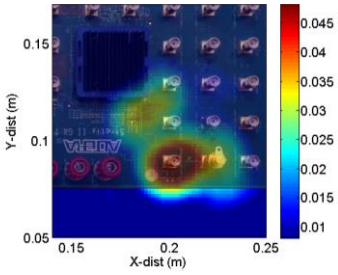

Fig. 15. Focused field magnitude on the PCB plane without termination.

As Fig. 15 indicates, there are two sources of radiation – the FPGA heat sink and SMA connectors. Due to the non-termination of the active differential lines, a common mode current was generated on the traces and radiated from nearby structures, such as the heatsink cavity and the SMA connector.

III. CONCLUSION

The first step in mitigating EMI involves identifying the source of radiation on the DUT, which allows a much more effective solution to be applied. The emission source microscopy technique presented in this paper can help not only to approximately identify the sources of radiation on the PCB, but also to quantify the effect of EMI mitigation techniques on the particular source. This can lead to improved, more cost-effective EMI mitigation solutions.

ACKNOWLEDGMENT

This material is based upon work supported by the National Science Foundation under Grant No. 0855878.

REFERENCES

[1] P.L. Ransom, R. Mitra, "A method of locating defective elements in large phased arrays," *Proc. of the IEEE*, vol. 59, no. 6, pp. 1029-1030, June 1971.

[2] K.S. Farhat, N. William, "Microwave holography applications in antenna development," *IEE Colloquium on Novel Antenna Measurement Techniques*, pp. 3/1, 3/4, 26, January 1994.

[3] D. Sheen, D. McMakin, T. Hall, "Three-dimensional millimeter-wave imaging for concealed weapon detection," in *IEEE Transactions on Microwave Theory and Techniques*, vol. 49, no. 9, September 2001.

[4] M. Fallahpour, J.T. Case, M. Ghasr, and R. Zoughi, "Piecewise and Wiener Filter-Based SAR Techniques for Monostatic Microwave Imaging of Layered Structures," in *IEEE Transactions on Antennas and Propagation*, vol. 62, no. 1, pp. 1-13, Jan. 2014.

[5] M. Fallahpour, M. Ghasr, J.T. Case, and R. Zoughi, "A Wiener Filter-Based Synthetic Aperture Radar (SAR) Algorithm for Microwave Imaging of Targets in Layered Media," in *Materials Evaluation*, vol. 69, no. 10, pp. 1227-1237, Oct. 2011.

[6] C.A. Balanis, "Antenna theory: Analysis and design," 3rd Edition, April 2005.

[7] A.D. Yaghjian, "An overview of near-field antenna measurements," *IEEE Transactions on Antennas and Propagation*, vol. ap-34, no. 1, January 1986.

[8] W.M. Brown, "Synthetic Aperture Radar," *IEEE Transactions on Aerospace and Electronic Systems*, vol. AES-3, no. 2, pp. 217-229, March 1967.

[9] J.T. Case, M.T. Ghasr, R. Zoughi, "Optimum two-dimensional uniform spatial sampling for microwave SAR-based NDE imaging," *IEEE Transactions on Instrumentation and Measurement*, vol. 60, no. 12, pp. 3806-3815, December 2011.

[10] H. Kajbaf, J.T. Case, Z. Yang, Y.R. Zheng, "Compressed sensing for SAR-based wideband three-dimensional microwave imaging system using non-uniform fast Fourier transform," *Radar, Sonar & Navigation*, IET , vol. 7, no. 6, pp. 658-670, July 2013.

[11] M. Abramowitz, M.W. Davidson, "Microscope objectives: Numerical aperture and resolution," *Molecular Expressions: Optical Microscopy Primer* (website), Florida State University, April, 2004.

[12] CST Microwave studio. [Online]. Available: http://www.cst.com

[13] G. Muchaidze, J. Koo, Q. Cai, T. Li, L. Han, A. Martwick, K. Wang, J. Min, J. L. Drewniak, D. Pommerenke, "Susceptibility scanning as a failure analysis tool for system-level electrostatic discharge (ESD) problems," *IEEE Transactions on Electromagnetic Compatibility*, vol. 50, no. 2, pp. 268-276, May 2008.